



**Please cite the Published Version**

Petrican, Raluca , Chopra, Sidhant, Murgatroyd, Christopher  and Fornito, Alex (2024) Sex-differential markers of psychiatric risk and treatment response based on premature aging of functional brain network dynamics and peripheral physiology. *Biological Psychiatry*. ISSN 0006-3223

**DOI:** <https://doi.org/10.1016/j.biopsych.2024.10.008>

**Publisher:** Elsevier BV

**Version:** Accepted Version

**Downloaded from:** <https://e-space.mmu.ac.uk/636268/>

**Usage rights:**  [Creative Commons: Attribution 4.0](https://creativecommons.org/licenses/by/4.0/)

**Additional Information:** This is an open access article which first appeared in *Biological Psychiatry*, published by Elsevier

**Data Access Statement:** The raw data are available at <https://nda.nih.gov/ccf/lifespan-studies> (HCP-A) and at <https://nda.nih.gov/ccf/disease-studies> (PDC, HCP-EP) upon completion of the relevant data use agreements. The data used in this report came from the Lifespan Human Connectome Project-Aging Annual Release 2.0 (NDA Collection ID 2847), DOI: 10.15154/1520707. The HCP-EP (NDA Collection ID 2914) 1.1 Release data used in this report came from DOI: 10.15154/1522899. The PDC data (NDA Collection ID 2844) used in this report came from Data Release 1.0, DOI: <https://doi.org/10.15154/1528673>.

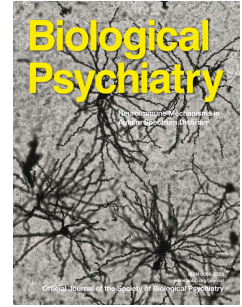
**Enquiries:**

If you have questions about this document, contact [openresearch@mmu.ac.uk](mailto:openresearch@mmu.ac.uk). Please include the URL of the record in e-space. If you believe that your, or a third party's rights have been compromised through this document please see our Take Down policy (available from <https://www.mmu.ac.uk/library/using-the-library/policies-and-guidelines>)

# Journal Pre-proof

Sex-differential markers of psychiatric risk and treatment response based on premature aging of functional brain network dynamics and peripheral physiology

Raluca Petrican, Sidhant Chopra, Christopher Murgatroyd, Alex Fornito



PII: S0006-3223(24)01667-6

DOI: <https://doi.org/10.1016/j.biopsych.2024.10.008>

Reference: BPS 15627

To appear in: *Biological Psychiatry*

Received Date: 21 June 2024

Revised Date: 16 September 2024

Accepted Date: 6 October 2024

Please cite this article as: Petrican R., Chopra S., Murgatroyd C. & Fornito A., Sex-differential markers of psychiatric risk and treatment response based on premature aging of functional brain network dynamics and peripheral physiology, *Biological Psychiatry* (2024), doi: <https://doi.org/10.1016/j.biopsych.2024.10.008>.

This is a PDF file of an article that has undergone enhancements after acceptance, such as the addition of a cover page and metadata, and formatting for readability, but it is not yet the definitive version of record. This version will undergo additional copyediting, typesetting and review before it is published in its final form, but we are providing this version to give early visibility of the article. Please note that, during the production process, errors may be discovered which could affect the content, and all legal disclaimers that apply to the journal pertain.

© 2024 Published by Elsevier Inc on behalf of Society of Biological Psychiatry.

1 Running head: CARDIOMETABOLIC AGING, BRAIN FLEXIBILITY, AND  
2 PSYCHOPATHOLOGY

3

4 Sex-differential markers of psychiatric risk and treatment response based on premature aging  
5 of functional brain network dynamics and peripheral physiology

6 Raluca Petrican<sup>1</sup>, Sidhant Chopra<sup>2,3,4</sup>, Christopher Murgatroyd<sup>5</sup>, & Alex Fornito<sup>6</sup>

7

8 <sup>1</sup>Institute of Population Health, Department of Psychology, University of Liverpool, Bedford  
9 Street South, Liverpool, L69 7ZA, UK. <sup>2</sup>Department of Psychology, Yale University, New  
10 Haven, USA. <sup>3</sup>Department of Psychiatry, Brain Health Institute, Rutgers University,  
11 Piscataway, USA. <sup>4</sup>Orygen, Parkville, Australia. <sup>5</sup>Department of Life Sciences, Manchester  
12 Metropolitan University, Manchester, UK. <sup>6</sup>The Turner Institute for Brain and Mental Health,  
13 School of Psychological Sciences, and Monash Biomedical Imaging, Monash University,  
14 Melbourne, VIC, Australia. Corresponding author email address:  
15 [raluca.petrican@liverpool.ac.uk](mailto:raluca.petrican@liverpool.ac.uk) (R.P.).

16 **Conflict of interest.** The authors report no biomedical financial interests or potential  
17 conflicts of interest.

18 **Acknowledgments.** Data used in the preparation of this article were obtained from the  
19 Lifespan Human Connectome Project (HCP) ([https://www.](https://www.humanconnectome.org/study/hcp-lifespan-aging)  
20 [humanconnectome.org/study/hcp-lifespan-aging](https://www.humanconnectome.org/study/hcp-lifespan-aging) ), the Perturbation of the Depression  
21 Connectome (PDC, Data Release 1.0), and the Human Connectome Project-Early Psychosis  
22 (HCP-EP, Data Release 1.1), all of which are held in the NIMH Data Archive (NDA). The  
23 Lifespan HCP research is supported by grants U01MH109589 , U01MH109589-S1 ,  
24 U01AG052564 , and U01AG052564-S1 and by the 14 NIH Institutes and Centers that  
25 support the NIH Blueprint for Neuroscience Research , by the McDonnell Center for Systems

26 Neuroscience at Washington University, by the Office of the Provost at Washington  
27 University, by the University of Minnesota Medical School, by the University of  
28 Massachusetts Medical School, and by the University of California Los Angeles Medical  
29 School. The PDC research is supported by grant U01MH110008 from the NIMH. Research  
30 using Human Connectome Project for Early Psychosis (HCP-EP) data reported in this  
31 publication was supported by the National Institute of Mental Health of the National  
32 Institutes of Health under Award Number U01MH109977. This manuscript reflects the  
33 views of the authors and may not reflect the opinions or views of the NIH, HCP or PDC  
34 consortium investigators. AF was supported by the National Health and Medical Research  
35 Council (ID: 1197431) and Australian Research Council (ID: FL220100184).

36 Abstract

37 Background

38 Aging is a multilevel process of gradual decline that predicts morbidity and mortality.  
39 Independent investigations have implicated senescence of brain and peripheral physiology in  
40 psychiatric risk, but it is unclear whether these effects stem from unique or shared  
41 mechanisms.

42 Methods

43 To address this question, we analyzed clinical, blood chemistry and resting state functional  
44 neuroimaging data in a healthy aging cohort (N= 427; age 36-100 years) and two disorder-  
45 specific samples encompassing patients with early psychosis (100 patients, 16-35 years) and  
46 major depressive disorder (MDD) (104 patients, 20-76 years).

47 Results

48 We identified sex-dependent coupling between blood chemistry markers of metabolic  
49 senescence (i.e., homeostatic dysregulation), functional brain network aging, and psychiatric  
50 risk. In females, premature aging of frontoparietal and somatomotor networks was linked to  
51 greater homeostatic dysregulation. It also predicted the severity and treatment resistance of  
52 mood symptoms (depression/anxiety [all three samples], anhedonia [MDD]) and social  
53 withdrawal/behavioral inhibition (avoidant personality disorder [healthy aging]; negative  
54 symptoms [early psychosis]). In males, premature aging of the default mode, cingulo-  
55 opercular, and visual networks was linked to reduced homeostatic dysregulation and  
56 predicted severity and treatment resistance of symptoms relevant to hostility/aggression  
57 (antisocial personality disorder [healthy aging]; mania/positive symptoms [early psychosis]),  
58 impaired thought processes (early psychosis, MDD) and somatic problems (healthy aging,  
59 MDD).

60 Conclusions

61 Our findings identify sexually dimorphic relationships between brain dynamics, peripheral  
62 physiology, and risk for psychiatric illness, suggesting that the specificity of putative risk  
63 biomarkers and precision therapeutics may be improved by considering sex and other  
64 relevant personal characteristics.

65 *Keywords:* cardiometabolic aging; functional brain network flexibility; sex differences;  
66 psychosis; major depressive disorder.

67

Journal Pre-proof

68           Aging is an intricate biological process of gradual decline that unfolds across multiple  
69 interconnected levels within a living organism (1, 2). Biological senescence can thus be  
70 measured at multiple scales, from cellular indices of altered gene expression to organism-  
71 level biomarkers of cardiometabolic functioning (1, 3, 4). Although biological senescence  
72 tracks with chronological age, trajectories of decay show considerable inter-individual  
73 variability as a function of time since birth, with more advanced biological, relative to  
74 chronological, age emerging as a critical predictor of morbidity and mortality (4-6).

75           A rapidly growing literature underscores the relevance of biological senescence to  
76 both physical and psychological health outcomes across the lifespan. For instance, genetic  
77 risk for metabolic dysfunction is linked to poorer cognitive performance in childhood (7),  
78 while lifestyle factors supportive of cardiometabolic health (e.g., exercise) alleviate cognitive  
79 and brain decline in older adulthood (7-10). The interdependence of these and other systems  
80 means that the combined use of physiological and brain indicators of aging yields the most  
81 accurate prediction of cognitive functioning from midlife onwards (5, 11-13).

82           Differences in cardiometabolic and brain aging between neurotypical and psychiatric  
83 populations are gaining increasing attention as a potential gateway to understanding and  
84 treating mental ill-health. Extant evidence implicates premature cardiometabolic and  
85 structural brain aging in the pathophysiology of anxiety (14-17), major depressive disorder  
86 (MDD) (15, 16, 18) and psychosis spectrum disorders (19-23). Conversely, greater structural  
87 brain similarity to MDD and psychosis among healthy individuals is related to poorer  
88 cardiometabolic health and mental processing (24).

89           The evidence reviewed above comes mainly from independent investigations of  
90 premature structural brain aging and cardiometabolic senescence. This work has linked brain  
91 aging to diagnoses of anxiety, MDD, and psychosis (16, 22), with cardiometabolic aging only  
92 linked to specific symptoms, such as anxious fatigue and blunted reward responsiveness in

93 MDD (25-28) or negative symptoms in psychosis (29). It is therefore unclear whether  
94 premature brain and cardiometabolic senescence have unique or shared connections with  
95 mental health, at the disorder and/or symptom level, and whether any such connections show  
96 continuity across the subclinical-to-clinical spectrum. It is also unclear whether the robustly  
97 documented sex differences in vulnerability to psychopathology (30-38) may (partially) stem  
98 from distinct patterns of overlap between sex-specific and cardiometabolic senescence-  
99 related brain patterns (30-38). The answers to these questions have critical implications for  
100 the design of personalized psychiatry interventions targeting sub-optimal aging trajectories in  
101 a multilevel (i.e., psychological and physical health), domain-specific, and/or sex-differential  
102 manner.

103         The present study focused on brain aging patterns correlated with cardiometabolic  
104 senescence and probed their relevance to mental well-being across the subclinical-to-clinical  
105 spectrum, including their power to explain sex differences in psychiatric risk (see Figure 1 for  
106 a schematic representation of our model). To this end, we analysed data from a healthy aging  
107 cohort (i.e., Human Connectome Project-Aging [HCP-A]) and two disorder-specific samples,  
108 encompassing early psychosis (i.e., HCP-EP) and MDD (i.e., Perturbation of the Depression  
109 Connectome [PDC]) patients. Our objectives were two-fold. First, among the HCP-A  
110 participants, we sought to identify how sexually dimorphic patterns of yoked cardiometabolic  
111 and brain aging are linked to subclinical variations in psychiatric symptoms. Given prior  
112 literature (25-28), we expected that premature brain and cardiometabolic senescence would  
113 be related to symptoms associated with internalizing disorders. Second, within each of our  
114 two psychiatric diagnosis-specific samples, we examined whether the neural aging patterns  
115 linked to cardiometabolic senescence and subclinical variations in disorder-specific  
116 symptoms in the HCP- A cohort predicted symptom severity and/or treatment-resistance in  
117 psychosis and/or MDD (25-29).



118

## Methods and Materials

### 119 **Participants**

120 Our analyses leveraged three publicly available datasets, the Human Connectome  
121 Project-Aging (HCP-A) (N = 427, 233 females, age range 36-100 years), Human  
122 Connectome Project-Early Psychosis (HCP-EP) (N = 77 non-affective [21 females] and 23  
123 affective [16 females] psychosis patients, age range 16-35 years) and Perturbation of the  
124 Depression Connectome (PDC) (N = 104 [59 females] severely depressed patients, age range  
125 20-76 years). All participants contributed complete data on all the scrutinised variables.  
126 Inclusion of data in the analyses was guided by the recommendations of the respective study  
127 teams. All three samples were predominantly White and right-handed (see Supplemental  
128 Information ([SI] A.1 for details).

### 129 **Cardiometabolic Aging**

130 In the BioAge R software package (<https://github.com/dayoonkwon/BioAge>), aging-  
131 related decline in cardiometabolic function within the HCP-A sample was quantified with  
132 three well-accepted and validated algorithms, Klemmera-Doubal method (KDM, (39)),  
133 homeostatic dysregulation(3), and PhenoAge (40), whose outputs predict mortality,  
134 morbidity and healthspan in younger and older adults (3-6, 39, 40). The KDM algorithm uses  
135 linear regression to predict chronological age from a set of biomarkers within a reference  
136 group. An individual's KDM biological age prediction corresponds to the chronological age  
137 at which their physiology would be normal in the reference group. The homeostatic  
138 dysregulation (thereafter dubbed "dyshomeostasis") algorithm applies Mahalanobis distance  
139 to a biomarker set to estimate the dissimilarity between an individual's physiology and the  
140 physiology of a healthy young adult (20-30 years) group. The PhenoAge algorithm uses an  
141 exponential function to predict mortality from a set of biomarkers in a reference group. An  
142 individual's PhenoAge biological age prediction corresponds to the chronological age at

143 which their mortality risk would be normal in the reference group. To quantify premature  
144 aging, we computed the difference between an individual's estimated age from each of KDM  
145 and PhenoAge algorithms and their chronological age (4, 41). Positive and negative values  
146 reflect premature and delayed cardiometabolic senescence, respectively. Due to the skewness  
147 of the raw dyshomeostasis score distribution, log-transformed scores outputted by the  
148 BioAge R package were used in all analyses. SI A.2 contains further details on the age  
149 prediction algorithms and the inputted biomarker set.

### 150 **Psychological Functioning**

151 In the HCP-A sample, psychological functioning was assessed via participants'  
152 responses on the DSM-oriented scales (Depression, Anxiety, Attention Deficit Hyperactivity  
153 Disorder [ADHD], Avoidant Personality, Antisocial Personality, Somatic Symptom  
154 Disorder) from the Achenbach Adult Self-Report (ASR) instrument for ages 18–59 (42). In  
155 the HCP-EP sample, positive, negative and cognitive psychotic symptoms were estimated  
156 based on Marder's (43) five-factor taxonomy of the Positive and Negative Symptom Scale  
157 (PANSS, (44)), while depressive and manic symptoms were measured using the  
158 Montgomery-Asberg Depression Rating Scale (MADRS, (45)) and the Young Mania Rating  
159 Scale (YMRS, (46)), respectively. Among the PDC patients, pre- and post-treatment  
160 depressive symptom severity was assessed with the Hamilton Depression Rating Scale  
161 (HDRS) (47) with a focus on the following HDRS subscales: Depressed Mood, Psychic  
162 Anxiety, Somatic Anxiety, Feelings of Guilt, Hypochondrias, Loss of Appetite, Weight Loss,  
163 Retardation, Agitation, Work and Activities, Libido, and Suicidal Tendencies. Changes in  
164 symptom severity were operationalized as the difference between standardized post-treatment  
165 (electroconvulsive therapy [ECT]: post-full series completion; ketamine treatment [KET]: 24  
166 hours post-last infusion; total sleep deprivation [TSD]: immediately after the overnight  
167 session) and standardized pre-treatment scores on the same HDRS subscale (see SI A.3 and

168 Table S2).

## 169 **Dynamic Functional Brain Architecture Related to Premature Cardiometabolic Aging**

170 **Functional connectivity and network-level analyses.** We analyzed resting state data  
171 already preprocessed using nearly identical pipelines by the HCP-A, HCP-EP and PDC study  
172 teams, respectively (cf. (48, 49), SI A 4.2). The concatenated preprocessed resting state runs  
173 were broken down into 30-s (i.e., 38 volumes) long non-overlapping windows. Across the  
174 three samples, network analyses were conducted on the same number of windows ( $N = 25$ )  
175 matching the duration of the sample with the least available data (PDC) (cf. (50-52), SI A  
176 4.3-4.4). Pairwise Pearson correlations between regional time series extracted from the  
177 Schaefer 300 parcel/17-network functional atlas (53-55) within each window were computed  
178 separately in Matlab (version 2022a) and expressed as Fisher's z-transformed scores.  
179 Negative scores were set to zero (cf. (56, 57), SI A 4.4). All the reported results were  
180 replicated with the Gordon atlas (58) (SI B).

181 The network-level metrics were computed with the Network Community Toolbox  
182 ((59)) (SI A 4.5). Window-specific community organisation was estimated with a multilayer  
183 generalized Louvain-like community detection algorithm (57, 60, 61). ROI-level variability  
184 in functional organisation was quantified using the "flexibility" function in the Network  
185 Community Toolbox as the number of times a given ROI changed functional communities  
186 between two consecutive windows. For each participant, the network analyses yielded a  
187 vector of 300 regional values indexing functional brain network flexibility (BNF).

### 188 ***Disorder and symptom-related brain network flexibility (BNF) maps.***

189 All the partial correlation analyses described below controlled for age, average  
190 relative scan-to-scan displacement, gender, site, race, handedness, antipsychotic medication  
191 dosage (HCP-EP only), as well as treatment group and delay [in days] between the pre- and  
192 post-treatment assessments (PDC only) (SI A.5, 7).

193 *HCP-A*. BNF maps linked to psychiatric disorder scores were computed via partial  
194 Spearman's correlations between ROI-specific BNF scores and scores on each of the six  
195 DSM-oriented scales from the ASR.

196 *HCP-EP*. Symptom-specific BNF maps were estimated via Spearman's partial  
197 correlation of ROI-specific network flexibility indices with the PANSS (positive, negative  
198 and cognitive) factors, YMRS mania and the MADRS depression scores across all  
199 participants.

200 *PDC*. To characterise the BNF correlates of overall MDD symptom severity at each  
201 time point, as well as depressive symptom change, partial Spearman's correlations were  
202 computed between the ROI-specific network flexibility and the HDRS scores at  
203 baseline/post-treatment, as well as the HDRS difference scores (post-treatment – pre-  
204 treatment).

## 205 **Statistical Analysis**

206 A discovery partial least squares (PLS) correlation analysis (62) with 10-fold cross-  
207 validation (SI A 6.1) identified BNF patterns related to sex and cardiometabolic senescence  
208 in the HCP-A sample. In this analysis, a robust correlation between the extracted BNF latent  
209 variable and sex/cardiometabolic senescence suggests that the former differs between males  
210 and females/depends on physiological aging measures. Conversely, the lack of a robust  
211 correlation implies that the BNF profile is common to males and females/unrelated to  
212 physiological aging measures. A robust correlation of the BNF latent variable with both sex  
213 and cardiometabolic senescence would indicate overlap between sex-specific and  
214 cardiometabolic senescence-related BNF patterns. The discovery PLS analysis was  
215 conducted on non-residualized data. However, the cross-validation partial correlation  
216 analyses linking the predicted values of the brain latent variable to sex, cardiometabolic  
217 senescence (Figure 2-B) or ROI-specific BNF scores (Figure 2-D) controlled for

218 chronological age in addition to site, race, handedness, and average relative scan-to-scan  
219 displacement (SI A.7). Because advancing age predicts greater cardiometabolic senescence  
220 (3, 4, 41) and BNF (63-66), a positive correlation between the cross-validated BNF latent  
221 variable and cardiometabolic senescence would imply that premature brain aging is linked to  
222 premature cardiometabolic senescence, whereas a negative correlation would imply that  
223 premature brain aging is linked to delayed cardiometabolic senescence (and vice versa).

224 Canonical correlation analyses (CCA) (67) probed the relationship between the partial  
225 correlation BNF maps linked to sex-cardiometabolic senescence in the HCP-A (Figure 2-D)  
226 and the BNF maps tracking psychiatric disorder scores in the same HCP-A sample (CCA 1),  
227 symptom severity in early psychosis (CCA 2) or MDD (CCA 3), respectively.

## 228 Results

### 229 Associations between Dyshomeostasis and Brain Network Flexibility are Sex-Specific

230 The discovery PLS analysis conducted in the full HCP-A sample revealed a single  
231 latent variable pair ( $p = .0002$ , shared variance of 73.75%). The cross-validated latent  
232 variable pair ( $r = .30$ , permutation-based  $p = 10^{-5}$ ) identified sexually dimorphic associations  
233 between BNF and dyshomeostasis, but not KDM/PhenoAge (Figure 2-A). Thus, greater  
234 dyshomeostasis, particularly among females, was related to greater Control and SM network  
235 flexibility, whereas reduced dyshomeostasis, particularly among males, was yoked to greater  
236 DMN, SAL, VIS and DAN network flexibility (Figure 2-A, B). The unique, additive  
237 contributions of sex and dyshomeostasis to the extracted brain latent variable (Figure 2-B)  
238 were confirmed through a linear regression analysis predicting the cross-validated BNF latent  
239 variable scores from sex, dyshomeostasis and the confounders listed in SI A.7 ( $bs$  of 2.08,  
240 95% CI = [1.25; 2.91] and .70, 95% CI = [.27; 1.16] for sex and dyshomeostasis,  
241 respectively).

242 In the following analyses, we examine the relevance of the cross-validated

243 dyshomeostasis-BNF profile (Figure 2-D) to BNF patterns tracking psychiatric symptoms in  
244 healthy aging, early psychosis and MDD. We predicted that the dyshomeostasis-BNF profile  
245 will correlate positively with symptoms mainly detected among females showing greater  
246 physiological aging (e.g., mood problems, anhedonia) (15, 20, 30, 33) and correlate  
247 negatively with symptoms primarily observed among physiologically “young” males (3)  
248 (e.g., aggressive behavior) (68).

249

### 250 **Sexually Dimorphic Associations Between Brain Network Flexibility and Subclinical** 251 **Internalizing and Externalizing**

252 A cross-validated CCA revealed a single statistically significant mode ( $r = .72$ ,  
253 permutation-based  $p = 10^{-5}$ , Figure 3-C) reflecting a positive association between BNF  
254 patterns linked to female dyshomeostasis and those tracking higher anxiety, avoidant  
255 personality, and depressive disorder scores across sexes (Figure 3-A, B) Conversely, there  
256 was a positive correlation between BNF patterns linked to reduced male dyshomeostasis and  
257 those related to higher antisocial and somatic personality disorder scores across sexes (Figure  
258 3-A, B).

259

### 260 **Dyshomeostasis-BNF Patterns are Related to Symptom Severity in Psychosis**

261 We next used CCA to investigate whether the dyshomeostasis-BNF profile from the  
262 HCP-A sample would relate to depressive and negative psychotic symptom severity in the  
263 HCP-EP patient data (25, 27, 29). The resultant cross-validated CCA variate pair ( $r = .56$ ,  
264 permutation-based  $p = 10^{-5}$ , Figure 4-C) unveiled a positive relationship between BNF  
265 patterns linked to female dyshomeostasis and those linked to depressive as well as negative  
266 symptoms in the HCP-EP sample (Figure 4-A, B). The extracted CCA mode also revealed  
267 that BNF patterns associated with reduced male dyshomeostasis overlapped with those

268 tracking manic and positive symptom severity in the HCP-EP (Figure 4-B).

269

270 **Dyshomeostasis-BNF Patterns Are Related to Treatment-Resistant Anxiety and**

271 **Anhedonia**

272 Finally, we probed the relationship between the dyshomeostasis-BNF profile from

273 HCP-A and BNF patterns correlated with overall MDD severity at each time point

274 (longitudinal  $r$  of .18]), as well as MDD symptom resistance following treatment. The

275 discovery CCAs unveiled a sole CCA variate pair, which was cross-validated across all 10

276 test folds ( $r = .82$ , permutation-based  $p = 10^{-5}$ , Figure 5-C). The identified mode positively

277 linked BNF patterns associated with female dyshomeostasis to those associated with greater

278 overall MDD severity after treatment, as well as treatment-resistant anhedonia (i.e.,

279 engagement with work and personal interests, libido), suicidal tendencies, agitation and

280 psychic anxiety (Figure 5-B). A positive association also emerged between BNF patterns

281 correlated with reduced male dyshomeostasis and those tracking treatment resistance in

282 appetite and retardation (i.e., mental and physical slowness) (Figure 5-B).

283

### Discussion

284 Prior research linked cardiometabolic aging to specific psychiatric symptoms and

285 brain aging to specific diagnoses (16, 22, 25-29). The present study indicates that sex-

286 differential patterns of functional brain dynamics linked to metabolic senescence, specifically,

287 dyshomeostasis (3), predict vulnerability to psychopathology in healthy aging, as well as the

288 occurrence and treatment resistance of individual symptoms in two clinical groups. The

289 identified neural profiles, suggestive of premature vs delayed functional aging (i.e., greater vs

290 lower BNF, (63-66)) spanned networks implicated in psychopathology broadly (69), as well

291 as those related specifically to the two disorders under scrutiny (70-77). The unique

292 association between BNF patterns and dyshomeostasis, but not KDM or PhenoAge, indices

293 of premature aging suggests that sex-dependent psychiatric vulnerability is related to absolute  
294 distance from the optimal “young adult” cardiometabolic profile rather than rate of decline  
295 relative to peers of the same chronological age. Whether the null effects observed for KDM  
296 and PhenoAge stem from the greater heterogeneity of the associated functional brain profiles  
297 is a question worth probing in the future.

298         Recent studies have begun to unravel the sex-dependent molecular and functional  
299 brain pathways underpinning global psychopathology risk (37), and differential risk for  
300 externalizing vs internalizing problems (34). Complementing this work, we document the  
301 divergent, sex-dependent relationship of metabolic senescence and associated BNF patterns  
302 with risk for internalizing vs externalizing psychopathology in typical aging. Specifically,  
303 among the healthy adults from HCP-A, BNF patterns related to female dyshomeostasis (i.e.,  
304 higher Control and SM, but lower DMN, SAL, DAN and VIS, BNF) overlapped those  
305 tracking depression, anxiety and avoidant personality disorder symptoms across sexes (see  
306 Figure 3-B). Complementarily, BNF patterns linked to reduced male dyshomeostasis (i.e.,  
307 greater DMN, SAL, DAN and VIS, but lower Control and SM BNF) overlapped those  
308 tracking antisocial personality and somatic disorder symptoms. Broadly, our results fit well  
309 with extant evidence and evolutionary theory connecting internalizing psychopathology to  
310 “diseased”-like states associated with high inflammation (78-80) and connecting  
311 externalizing behaviours to physical attributes and neuroendocrine responses that tend to  
312 typify younger males in good health (68). The sex-dependent association between premature  
313 metabolic senescence and depression/anxiety disorders further aligns with evidence that  
314 females show more intense and prolonged responses to stressors compared to males (30, 33,  
315 36).

316         Premature female and delayed male senescence were linked to opposite patterns of  
317 DMN-SM functional stability (i.e., lower BNF), which accords with prior reports linking



318 older (relative to younger) adulthood to more dwell time in brain states dominated by internal  
319 mentation rather than sensory and SM networks (81). The link between depression/anxiety  
320 disorder scores and greater DMN (rather than Control or SM) stability is consonant with  
321 extant evidence that the severity of internalizing psychopathology tracks with relative DMN  
322 (over Control and SM) functional dominance (i.e., comparatively greater connectivity  
323 strength, as well as higher frequency and more time spent in DMN-dominated states) (82,  
324 83).

325         The association between externalizing risk and lower functional stability in DMN and  
326 VIS, two networks involved in perceiving and creating mental representations of contextual  
327 information (84-86), resonates with recent proposals implicating deficient processing of  
328 contextual information in the pathology of antisocial personality disorders (87). Likewise, the  
329 correlation between predisposition towards externalizing disorders and greater BNF in SAL,  
330 a network linked to transdiagnostic deficits in cognitive control (69), is in line with extant  
331 theory and evidence on the importance of inhibitory resources in antisocial personality  
332 disorders (88, 89).

333         Beyond disorder-level associations with internalizing vs externalizing risk, the sex-  
334 dependent BNF profile linked to metabolic senescence also showed symptom-specific  
335 relationships. Thus, the brain patterns yoked to age-premature female dyshomeostasis, as  
336 well as depression, anxiety and avoidant personality disorders in HCP-A, were associated  
337 with BNF patterns tracking severity and treatment resistance of symptoms related to mood  
338 (depression [HCP-EP, PDC], anxiety [PDC], anhedonia [PDC]) and social  
339 withdrawal/behavioral inhibition (negative psychotic symptoms [HCP-EP]) (42, 43). These  
340 findings extend prior research linking cardiometabolic dysfunction and inflammation to  
341 negative and depressive symptoms in psychosis (29, 90), as well as anxious fatigue (28) and  
342 anhedonia (25) in MDD. Our results also could also advance existing efforts to differentiate

343 psychosis spectrum pathologies and predict responsiveness to treatment based on cellular  
344 senescence, as well as structural and functional brain indices associated with specific  
345 symptom types (91-93). The involvement of the BNF profile linked to female dyshomeostasis  
346 in negative symptoms dovetails nicely with reports of greater cellular senescence among  
347 females diagnosed with psychosis spectrum disorders (38). Its relevance to the post-treatment  
348 persistence of anhedonia further resonates with evidence on sex differences in the normative  
349 development of reward processing skills (31) and as observed in MDD (35).

350         The BNF patterns linked to reduced male dyshomeostasis (i.e., greater DMN, SAL,  
351 DAN and VIS, but lower Control and SM, BNF), as well as antisocial personality and  
352 somatic problems in healthy aging, correlated positively with the severity of mania and  
353 positive psychotic symptoms, in which externalizing features, such as hostility and aggressive  
354 behaviour, are prominent (43, 46). This finding echoes prior reports linking familial risk for  
355 psychosis to delayed cellular senescence (94), as well as evidence implicating greater DMN  
356 (over SM) BNF (95) and atypical VIS network connectivity and processing in the pathology  
357 of psychosis disorders (96-98). The relationship between mania severity and BNF patterns  
358 linked to reduced male dyshomeostasis sheds further light on the proposed role of metabolic  
359 overdrive in the pathophysiology of manic episodes (99). Specifically, in younger patient  
360 samples such as the HCP-EP, the higher metabolic rate conducive to systemic dysregulation  
361 in the long run may lend the appearance of greater physiological youth, either directly or via  
362 associated behaviours, such as heightened physical activity levels (99).

363         The brain patterns related to delayed male metabolic senescence further overlapped  
364 with those tracking treatment resistance for appetite and impaired/slowed thought processes  
365 in MDD. This association with appetite resonates with the relevance of the male homeostasis-  
366 BNF profile to somatic symptoms in the HCP-A sample. Given the transdiagnostic relevance  
367 of impaired thought processes, likely linked to deficient cognitive control (69), the findings

368 involving the reduced male dyshomeostasis-BNF patterns in HCP-EP and PDC are consistent  
369 with reports that individuals at clinical risk for psychosis have multiple comorbidities (100),  
370 which is reflected in the substantial number of deficient brain pathways shared between  
371 psychosis and multiple psychiatric and neurological disorders (101).

## 372 **Limitations and Future Directions**

373 Aging is a multilevel process (1) and investigations combining markers of cellular  
374 (e.g., DNAm, (102) and organism-level cardiometabolic senescence as those used here could  
375 improve measurement sensitivity and accuracy (14, 103-108). Moreover, structural and  
376 functional brain aging show distinguishable trajectories, which, in turn, are differentially  
377 associated with mood and psychotic pathology (18, 109-113). Future cross-species studies  
378 incorporating pharmacological and/or experimental manipulations of mood and psychotic  
379 symptoms while collecting (quasi-)contemporaneous assessments of multiple structural (e.g.,  
380 neurogenesis rate, gray matter volume, white matter microstructure) and functional indices of  
381 brain aging, including behavioural and neural responses to clinically relevant task contexts  
382 (e.g., linked to impulsivity or reward sensitivity) could help provide a more comprehensive  
383 characterization of the effects herein reported. Such investigations could further shed light on  
384 the specific neurotransmitter systems and neuronal (inhibitory, excitatory) vs non-neuronal  
385 (e.g., astrocytes), cell types likely to bridge mental health, as well as cardiometabolic and  
386 brain senescence (21, 29, 104, 114, 115). Cellular and organism-level senescence can be  
387 accelerated by environmental adversity (107, 116-120) and maladaptive lifestyle choices  
388 (e.g., lack of regular exercise (9, 20), poor diet (121, 122)). Cross-species research which  
389 manipulates exposure to environmental adversity and lifestyle factors, such as aerobic  
390 exercise and diet, could help elucidate the “driver” behind the inter-relationships among sex-  
391 differential patterns of cellular and organism-level senescence, structural/functional brain  
392 aging and vulnerability to internalizing/externalizing psychopathology.

393 Our analyses focused on blood-chemistry-derived measures of physiological aging as  
394 these are highly predictive of cardiometabolic outcomes (123). However, the development of  
395 DNA methylation (DNAm) aging algorithms, termed “clocks”, has much potential. While  
396 first-generation DNAm clocks were developed to predict chronological age and were less  
397 sensitive to cardiometabolic aging compared to blood-chemistry–derived measures (124),  
398 newer DNAm clocks, developed to predict mortality, could be fine-tuned to dissect  
399 multimorbidity within cardiometabolic diseases and the impact of different lifestyle factors.

400 The predominantly cross-sectional design of our study limits causal inferences. The  
401 sample's demographic composition, being predominantly White and right-handed, may affect  
402 the generalizability of the findings. Longitudinal investigations with more diverse  
403 populations are needed to better understand the temporal dynamics and universality of brain-  
404 metabolic aging associations. For instance, examination of cardiometabolic senescence in  
405 socioeconomically diverse samples of children and adolescents could be instrumental in  
406 identifying and facilitating early amelioration of suboptimal brain maturation trajectories  
407 likely to enhance vulnerability to psychopathology. Such work is well-justified considering  
408 evidence that the functional impact of modifiable risk factors (e.g., exercise, diet) is stronger  
409 in earlier life (125). Similarly, future research could extend our analyses on the independent  
410 additive contributions of sex and cardiometabolic senescence to brain network flexibility by  
411 directly testing for or using genetic strategies (e.g., Mendelian randomization, (126)) to parse  
412 causal interactions between these variables.

413 We did not have sufficient statistical power to probe treatment-specific effects on the  
414 brain patterns associated with cardiometabolic senescence. Such research is worth pursuing  
415 since different treatments impact distinct physiological systems (127-132) and patterns of  
416 neuroplasticity (133, 134), which, in turn, are likely to show distinguishable associations with  
417 cellular and organism-level markers of senescence. The potential modulatory effects of

418 ongoing and lifetime psychotropic medication use on treatment response also warrant further  
419 study.

420 We used three publicly available datasets (HCP-A, HCP-EP and PDC) to reveal  
421 convergent patterns of association between BNF profiles linked to physiological aging and  
422 psychiatric symptoms. While corresponding measures showed substantial conceptual overlap,  
423 further efforts should be made to harmonize data collection methods to improve the  
424 consistency and comparability of findings.

#### 425 **Conclusions**

426 We identified a multimodal marker of metabolic and functional brain network  
427 senescence predictive of psychiatric disorder- and symptom-level vulnerability. By  
428 characterizing complementary, sex-dependent patterns of neurobiological aging that predict  
429 mental health outcomes, our investigation can act as a springboard for future research into the  
430 mechanisms underpinning sex differences in risk for internalizing vs externalizing disorders,  
431 as well as those accounting for sex differences in the burden of psychotic and depressive  
432 symptoms.

433

434 **Materials & Correspondence.** Correspondence and material requests should be addressed to  
435 R.P. (raluca.petrican@liverpool.ac.uk).

436 **Data statement.** The raw data are available at <https://nda.nih.gov/ccf/lifespan-studies> (HCP-  
437 A) and at <https://nda.nih.gov/ccf/disease-studies> (PDC, HCP-EP) upon completion of the  
438 relevant data use agreements. The data used in this report came from the Lifespan Human  
439 Connectome Project-Aging Annual Release 2.0 (NDA Collection ID 2847), DOI:  
440 [10.15154/1520707](https://doi.org/10.15154/1520707). The HCP-EP (NDA Collection ID 2914) 1.1 Release data used in this  
441 report came from DOI: [10.15154/1522899](https://doi.org/10.15154/1522899). The PDC data (NDA Collection ID 2844) used in  
442 this report came from Data Release 1.0, DOI: <http://dx.doi.org/10.15154/1528673>.

443 **Code availability.** We used already existing code, as specified in the main text with links for  
444 free download.

445

446

447 **Supplement Description:**

448

449 Supplemental Methods, Results, Tables S1-S2, and Figures S1-S6

450

## 451 Figure Captions

452 *Figure 1.* Schematic representation of our framework. Panel A: The KDM algorithm uses  
453 linear regression to predict chronological age from a set of biomarkers within a reference  
454 group. An individual's KDM biological age prediction corresponds to the chronological age  
455 at which their physiology would be normal in the reference group. The PhenoAge algorithm  
456 uses an exponential function to predict mortality from a set of biomarkers in a reference  
457 group. An individual's PhenoAge biological age prediction corresponds to the chronological  
458 age at which their mortality risk would be normal in the reference group. Indices of  
459 premature aging are computed by subtracting from an individual's age estimate as outputted  
460 by the KDM and PhenoAge algorithms, respectively, from an individual's chronological age.  
461 Positive and negative indices reflect premature and delayed cardiometabolic senescence,  
462 respectively. Panel (B): The homeostatic dysregulation algorithm applies Mahalanobis  
463 distance to a biomarker set in order to estimate the dissimilarity between an individual's  
464 physiology and the physiology of a healthy (overall physically fit) young adult (20-30 years)  
465 group. Individuals with reduced homeostatic dysregulation (represented by the gray circle)  
466 have a physiological profile relatively *more similar* to that of the young adult reference  
467 group, whereas those with greater homeostatic dysregulation (represented by the red circle)  
468 have a physiological profile relatively *more dissimilar* to that of the young adult reference  
469 group. Panel (C): BNF was computed for each ROI in the Schaefer300-17 Networks atlas as  
470 the number of times it changed functional community affiliation (shown as differently  
471 coloured shades) between two consecutive non-overlapping time windows. For ease of  
472 interpretation, BNF scores are described in reference to the ROI's network affiliation in the  
473 Schaefer atlas. The subnetworks from the Schaefer 17-network atlas (e.g., Control A/B/C)  
474 have been combined into one to increase comparability with the Gordon atlas. In panels (D)-  
475 (F), disorders or symptoms expected to correlate with cardiometabolic and brain aging are in

476 black font, whereas those scrutinised on an exploratory basis and to establish the specificity  
477 of any observed effects are in grey font. Panel (F): Correlated patterns of change in BNF and  
478 clinical symptoms assessed before and after treatment with ECT, ketamine or sleep  
479 deprivation in a sample of MDD patients. Premature cardiometabolic aging, estimated in  
480 reference to one's chronological age (A) or a healthy young adult sample (B) was posited to  
481 predict, in a sex-differential manner, patterns of functional brain network aging (i.e., BNF)  
482 (C). The latter were hypothesized to explain sex-differential subclinical variations  
483 internalizing vs externalizing disorder symptoms in healthy aging (D), as well as severity and  
484 treatment-resistance of specific symptoms along the internalizing/negative to positive  
485 symptom spectrum in early psychosis (E) and MDD (F), respectively. BNF = brain network  
486 flexibility. ROI = region-of-interest. ECT = electroconvulsive therapy. MDD = major  
487 depressive disorder. Schaefer networks: TP= temporo-parietal. SAL-VAN = salience/ventral  
488 attention. LB = limbic. DMN = default mode. DAN = dorsal attention. SM-A =somatomotor-  
489 A. SM-B =somatomotor-B. VIS = visual.

490 *Figure 2.* The brain latent variable from the behavioral-PLS analysis linking sex and  
491 cardiometabolic aging to BNF in the HCP-A sample. Panel (A) shows the correlations of the  
492 sex and cardiometabolic aging variables with the brain latent variable scores in the discovery  
493 PLS analysis. Panel (B) shows the correlations of the sex and homeostatic dysregulation  
494 variables with the predicted brain latent variable scores (based on the 10-fold cross-validation  
495 procedure). Error bars are the 95% bootstrapped confidence intervals (described in SI A 6.1),  
496 as conducted in the discovery (panel A) and cross-validation (panel B) PLS analyses.  
497 Confidence intervals that do not include zero reflect robust correlations between the  
498 respective behavioral variable and the discovery (panel A) or predicted (panel B) brain latent  
499 variable score across all participants. Panel (C) depicts the ROI-specific weights/loadings on  
500 the brain latent variable identified with the discovery PLS analysis with a bootstrap ratio



501 greater than 2 in absolute value (cf. (135, 136)). These weights reflect the within-sample  
502 unique association between an ROI and the extracted brain latent variable after controlling  
503 for the association of the brain latent variable with all the other ROIs from the Schaefer atlas.  
504 Panel (D) depicts the Schaefer ROIs robustly correlated (based on cross-validated 99.9%  
505 confidence intervals, as described in SI A 6.1) with the predicted value of the brain latent  
506 variable from the cross-validation procedure. These are partial correlations controlling for  
507 chronological age, race, testing site, handedness and average motion per participant, as  
508 described in the main text under “Statistical Analysis” (PLS analysis section). These partial  
509 correlation coefficients between an ROI and the predicted value of the brain latent variable do  
510 not control for the correlation between the brain latent variable and the remaining Schaefer  
511 ROIs entered in the analysis. To facilitate interpretation, panels (E) and (F) present Schaefer  
512 network-based distributions of PLS weights (panel E) or partial correlations (panel F)  
513 summarizing the ROI-specific results from panels (C) and (D), respectively. The subnetworks  
514 from the Schaefer 17-network atlas (e.g., Control A/B/C) have been combined into one to  
515 increase comparability with the Gordon atlas. Error bars represent standard deviations. KDM  
516 = Klemere-Doubal Method. PLS = partial least squares. BNF = brain network flexibility. ROI  
517 = region-of-interest. Schaefer networks: TP= temporo-parietal. SAL-VAN = salience/ventral  
518 attention. LB = limbic. DMN = default mode. DAN = dorsal attention. SM-A =somatomotor-  
519 A. SM-B =somatomotor-B. VIS = visual.

520 *Figure 3.* Psychiatric disorder-specific BNF patterns linked by CCA to the homeostatic  
521 dysregulation-BNF profile identified in the same HCP-A sample (cf. Figure 2). Panel (A)  
522 depicts the cross-validated BNF patterns associated with sex and homeostatic dysregulation  
523 in the PLS analysis (cf. Figure 2-B, D). Unlike the brain maps in Figure 2-D, which are  
524 thresholded based on cross-validated 99.9% confidence intervals, the brain maps in panel  
525 (A), same as the disorder-BNF maps, are not thresholded. The CCA’s were run on

526 unthresholded brain maps in order to avoid any bias introduced by applying (somewhat)  
527 arbitrary statistical thresholds. The circular graph in panel (B) contains the correlation  
528 coefficients describing the relationship between the observed disorder-specific BNF scores  
529 and the predicted value of their corresponding canonical variate across all test CCAs. The  
530 shaded areas correspond to robust correlations observed in cross-validated CCAs featuring  
531 both Schaefer and Gordon atlas-based homeostatic dysregulation-BNF scores (see SI A 6.2  
532 for details on the 99.9% bootstrapped confidence intervals). Panel (C) contains the scatter  
533 plot describing the linear relationship between the predicted values of the homeostatic  
534 dysregulation-BNF profile from the PLS analysis (Figure 2) and the predicted psychiatric  
535 disorder-BNF profile from the cross-validation of the CCA 1 results. BNF = brain network  
536 flexibility. ROI = region-of-interest. Depress = Depression. ADHD = attention deficit  
537 hyperactivity disorder. Antisoc = antisocial personality disorder. Avoid = Avoidant  
538 personality disorder. Som = Somatic Disorder.

539 *Figure 4.* Early psychosis symptom-specific BNF patterns linked by CCA to the homeostatic  
540 dysregulation-BNF profile identified in the HCP-A sample (cf. Figure 2). Panel (A) depicts  
541 the cross-validated BNF patterns associated with sex and homeostatic dysregulation in the  
542 PLS analysis (cf. Figure 2-B, D). Unlike the brain maps in Figure 2-D, which are thresholded  
543 based on cross-validated 99.9% confidence intervals, the brain maps in panel (A), same as the  
544 symptom-BNF maps, are not thresholded. The CCA's were run on unthresholded brain maps  
545 in order to avoid any bias introduced by applying (somewhat) arbitrary statistical thresholds.  
546 The circular graph in panel (B) contains the correlation coefficients describing the  
547 relationship between the observed symptom-specific BNF scores and the predicted value of  
548 their corresponding canonical variate across all test CCAs. The shaded areas correspond to  
549 robust correlations observed in cross-validated CCAs based on both the Schaefer and Gordon  
550 atlas data (based on the bootstrapping-derived 99.9% confidence intervals). The shaded areas

551 on the brain images reflect the strength of the partial correlation between the BNF scores and  
552 psychotic symptoms (see the Method for the confounders controlled for in the partial  
553 correlation). Panel (C) contains the scatter plot describing the linear relationship between the  
554 predicted values of the homeostatic dysregulation-BNF profile from the PLS analysis (Figure  
555 2) and the predicted psychosis symptom-BNF profile from the cross-validation of the CCA 2  
556 results. PLS = partial least squares. CCA = canonical correlation analysis. BNF = brain  
557 network flexibility. ROI = region-of-interest.

558 *Figure 5.* BNF change patterns corresponding to treatment-related symptom change in MDD  
559 linked by CCA to the homeostatic dysregulation-BNF profile identified in the HCP-A sample  
560 (cf. Figure 2). Panel (A) depicts the cross-validated BNF patterns associated with sex and  
561 homeostatic dysregulation in the PLS analysis (cf. Figure 2-B, D). Unlike the brain maps in  
562 Figure 2-D, which are thresholded based on cross-validated 99.9% confidence intervals, the  
563 brain maps in panel (A), same as the symptom-BNF maps, are not thresholded. The CCA's  
564 were run on unthresholded brain maps in order to avoid any bias introduced by applying  
565 (somewhat) arbitrary statistical thresholds. The circular graph in panel (B) contains the  
566 correlation coefficients describing the relationship between the observed symptom-specific  
567 BNF (change) scores and the predicted value of their corresponding canonical variate across  
568 all test CCAs. The shaded areas correspond to robust correlations observed in cross-validated  
569 CCAs based on both the Schaefer and Gordon atlas data (based on the bootstrapping-derived  
570 99.9% confidence intervals). The shaded areas on the brain images reflect the strength of the  
571 partial correlation between pre-to-post treatment change in BNF and MDD symptoms (see  
572 the Method for the confounders controlled for in the partial correlation). Panel (C) contains  
573 the scatter plot describing the linear relationship between the predicted values of homeostatic  
574 dysregulation-BNF profile from the PLS analysis (Figure 2) and the MDD symptom  
575 (change)-BNF profile. PLS = partial least squares. CCA = canonical correlation analysis.

576 BNF = brain network flexibility. ROI = region-of-interest. Depress\_1 = total HDRS score  
577 (as described in the text) before treatment. Depress\_2 = total HDRS score (as described in the  
578 text) after treatment. Agit = agitation. Anx = psychic anxiety. Sadness = depressed mood.  
579 Hypoch= hypochondriasis. Slowed = retardation (thought-related/motor). Som = somatic  
580 anxiety. Work/Int = work/interests. HDRS = Hamilton Depression Rating Scale. MDD =  
581 Major Depressive Disorder.

Journal Pre-proof

582

## References

- 583 1. Belsky DW, Moffitt TE, Cohen AA, Corcoran DL, Levine ME, Prinz JA, et al.  
584 (2018): Eleven Telomere, Epigenetic Clock, and Biomarker-Composite Quantifications of  
585 Biological Aging: Do They Measure the Same Thing? *Am J Epidemiol*. 187:1220-1230.
- 586 2. Li X, Ploner A, Wang Y, Magnusson PK, Reynolds C, Finkel D, et al. (2020):  
587 Longitudinal trajectories, correlations and mortality associations of nine biological ages  
588 across 20-years follow-up. *Elife*. 9.
- 589 3. Cohen AA, Milot E, Yong J, Seplaki CL, Fulop T, Bandeen-Roche K, et al. (2013): A  
590 novel statistical approach shows evidence for multi-system physiological dysregulation  
591 during aging. *Mech Ageing Dev*. 134:110-117.
- 592 4. Levine ME (2013): Modeling the rate of senescence: can estimated biological age  
593 predict mortality more accurately than chronological age? *J Gerontol A Biol Sci Med Sci*.  
594 68:667-674.
- 595 5. Belsky DW, Caspi A, Houts R, Cohen HJ, Corcoran DL, Danese A, et al. (2015):  
596 Quantification of biological aging in young adults. *Proc Natl Acad Sci U S A*. 112:E4104-  
597 4110.
- 598 6. Belsky DW, Huffman KM, Pieper CF, Shalev I, Kraus WE (2017): Change in the Rate  
599 of Biological Aging in Response to Caloric Restriction: CALERIE Biobank Analysis. *J*  
600 *Gerontol A Biol Sci Med Sci*. 73:4-10.
- 601 7. Rashid B, Glasser MF, Nichols T, Van Essen D, Juttukonda MR, Schwab NA, et al.  
602 (2023): Cardiovascular and metabolic health is associated with functional brain connectivity  
603 in middle-aged and older adults: Results from the Human Connectome Project-Aging study.  
604 *Neuroimage*. 276:120192.

- 605 8. Soldan A, Pettigrew C, Zhu Y, Wang MC, Bilgel M, Hou X, et al. (2021): Association  
606 of Lifestyle Activities with Functional Brain Connectivity and Relationship to Cognitive  
607 Decline among Older Adults. *Cereb Cortex*. 31:5637-5651.
- 608 9. Tamman AJF, Koller D, Nagamatsu S, Cabrera-Mendoza B, Abdallah C, Krystal JH,  
609 et al. (2024): Psychosocial moderators of polygenic risk scores of inflammatory biomarkers  
610 in relation to GrimAge. *Neuropsychopharmacology*. 49:699-708.
- 611 10. Xu J, Hao L, Chen M, He Y, Jiang M, Tian T, et al. (2022): Developmental Sex  
612 Differences in Negative Emotion Decision-Making Dynamics: Computational Evidence and  
613 Amygdala-Prefrontal Pathways. *Cereb Cortex*. 32:2478-2491.
- 614 11. Shen C, Liu C, Qiu A (2023): Metabolism-related brain morphology accelerates aging  
615 and predicts neurodegenerative diseases and stroke: a UK Biobank study. *Transl Psychiatry*.  
616 13:233.
- 617 12. Wiesman AI, Rezich MT, O'Neill J, Morsey B, Wang T, Ideker T, et al. (2020):  
618 Epigenetic Markers of Aging Predict the Neural Oscillations Serving Selective Attention.  
619 *Cereb Cortex*. 30:1234-1243.
- 620 13. Zheng Y, Habes M, Gonzales M, Pomponio R, Nasrallah I, Khan S, et al. (2022):  
621 Mid-life epigenetic age, neuroimaging brain age, and cognitive function: coronary artery risk  
622 development in young adults (CARDIA) study. *Aging (Albany NY)*. 14:1691-1712.
- 623 14. Bourassa KJ, Garrett ME, Caspi A, Dennis M, Hall KS, Moffitt TE, et al. (2024):  
624 Posttraumatic stress disorder, trauma, and accelerated biological aging among post-9/11  
625 veterans. *Transl Psychiatry*. 14:4.
- 626 15. Gao X, Geng T, Jiang M, Huang N, Zheng Y, Belsky DW, et al. (2023): Accelerated  
627 biological aging and risk of depression and anxiety: evidence from 424,299 UK Biobank  
628 participants. *Nat Commun*. 14:2277.

- 629 16. Han LKM, Schnack HG, Brouwer RM, Veltman DJ, van der Wee NJA, van Tol MJ, et  
630 al. (2021): Contributing factors to advanced brain aging in depression and anxiety disorders.  
631 *Transl Psychiatry*. 11:402.
- 632 17. Kuan PF, Ren X, Clouston S, Yang X, Jonas K, Kotov R, et al. (2021): PTSD is  
633 associated with accelerated transcriptional aging in World Trade Center responders. *Transl*  
634 *Psychiatry*. 11:311.
- 635 18. Han LKM, Dinga R, Hahn T, Ching CRK, Eyer LT, Aftanas L, et al. (2021): Brain  
636 aging in major depressive disorder: results from the ENIGMA major depressive disorder  
637 working group. *Mol Psychiatry*. 26:5124-5139.
- 638 19. Constantinides C, Han LKM, Alloza C, Antonucci LA, Arango C, Ayesa-Arriola R, et  
639 al. (2023): Brain ageing in schizophrenia: evidence from 26 international cohorts via the  
640 ENIGMA Schizophrenia consortium. *Mol Psychiatry*. 28:1201-1209.
- 641 20. Damme KSF, Vargas TG, Walther S, Shankman SA, Mittal VA (2024): Physical and  
642 mental health in adolescence: novel insights from a transdiagnostic examination of FitBit  
643 data in the ABCD study. *Transl Psychiatry*. 14:75.
- 644 21. de Bartolomeis A, De Simone G, De Prisco M, Barone A, Napoli R, Beguinot F, et al.  
645 (2023): Insulin effects on core neurotransmitter pathways involved in schizophrenia  
646 neurobiology: a meta-analysis of preclinical studies. Implications for the treatment. *Mol*  
647 *Psychiatry*. 28:2811-2825.
- 648 22. Kaufmann T, van der Meer D, Doan NT, Schwarz E, Lund MJ, Agartz I, et al. (2019):  
649 Common brain disorders are associated with heritable patterns of apparent aging of the brain.  
650 *Nat Neurosci*. 22:1617-1623.
- 651 23. Lee J, Xue X, Au E, McIntyre WB, Asgariroozbehani R, Panganiban K, et al. (2024):  
652 Glucose dysregulation in antipsychotic-naïve first-episode psychosis: in silico exploration of  
653 gene expression signatures. *Transl Psychiatry*. 14:19.

- 654 24. Ma Y, Kvarta MD, Adhikari BM, Chiappelli J, Du X, van der Vaart A, et al. (2023):  
655 Association between brain similarity to severe mental illnesses and comorbid cerebral,  
656 physical, and cognitive impairments. *Neuroimage*. 265:119786.
- 657 25. Costi S, Morris LS, Collins A, Fernandez NF, Patel M, Xie H, et al. (2021): Peripheral  
658 immune cell reactivity and neural response to reward in patients with depression and  
659 anhedonia. *Transl Psychiatry*. 11:565.
- 660 26. Franklyn SI, Stewart J, Beaurepaire C, Thaw E, McQuaid RJ (2022): Developing  
661 symptom clusters: linking inflammatory biomarkers to depressive symptom profiles. *Transl*  
662 *Psychiatry*. 12:133.
- 663 27. Moriarity DP, Slavich GM, Alloy LB, Olinio TM (2023): Hierarchical Inflammatory  
664 Phenotypes of Depression: A Novel Approach Across Five Independent Samples and 27,730  
665 Adults. *Biol Psychiatry*. 93:253-259.
- 666 28. Stout DM, Simmons AN, Nievergelt CM, Minassian A, Biswas N, Maihofer AX, et al.  
667 (2022): Deriving psychiatric symptom-based biomarkers from multivariate relationships  
668 between psychophysiological and biochemical measures. *Neuropsychopharmacology*.  
669 47:2252-2260.
- 670 29. Wu Q, Long Y, Peng X, Song C, Xiao J, Wang X, et al. (2024): Prefrontal cortical  
671 dopamine deficit may cause impaired glucose metabolism in schizophrenia. *Transl*  
672 *Psychiatry*. 14:79.
- 673 30. Bangasser DA, Cuarenta A (2021): Sex differences in anxiety and depression: circuits  
674 and mechanisms. *Nat Rev Neurosci*. 22:674-684.
- 675 31. Barendse MEA, Swartz JR, Taylor SL, Fine JR, Shirtcliff EA, Yoon L, et al. (2024):  
676 Sex and pubertal variation in reward-related behavior and neural activation in early  
677 adolescents. *Dev Cogn Neurosci*. 66:101358.



- 678 32. Brown SJ, Christofides K, Weissleder C, Huang XF, Shannon Weickert C, Lim CK, et  
679 al. (2024): Sex- and suicide-specific alterations in the kynurenine pathway in the anterior  
680 cingulate cortex in major depression. *Neuropsychopharmacology*. 49:584-592.
- 681 33. Dark HE, Harnett NG, Hurst DR, Wheelock MD, Wood KH, Goodman AM, et al.  
682 (2022): Sex-related differences in violence exposure, neural reactivity to threat, and mental  
683 health. *Neuropsychopharmacology*. 47:2221-2229.
- 684 34. Dhamala E, Rong Ooi LQ, Chen J, Ricard JA, Berkeley E, Chopra S, et al. (2023):  
685 Brain-Based Predictions of Psychiatric Illness-Linked Behaviors Across the Sexes. *Biol*  
686 *Psychiatry*. 94:479-491.
- 687 35. Mansouri S, Pessoni AM, Marroquin-Rivera A, Parise EM, Tamminga CA, Turecki G,  
688 et al. (2023): Transcriptional dissection of symptomatic profiles across the brain of men and  
689 women with depression. *Nat Commun*. 14:6835.
- 690 36. Schilliger Z, Aleman-Gomez Y, Magnus Smith M, Celen Z, Meuleman B, Binz PA, et  
691 al. (2024): Sex-specific interactions between stress axis and redox balance are associated with  
692 internalizing symptoms and brain white matter microstructure in adolescents. *Transl*  
693 *Psychiatry*. 14:30.
- 694 37. Wendt FR, Pathak GA, Singh K, Stein MB, Koenen KC, Krystal JH, et al. (2023):  
695 Sex-Specific Genetic and Transcriptomic Liability to Neuroticism. *Biol Psychiatry*. 93:243-  
696 252.
- 697 38. Zhou J, Xia Y, Li M, Chen Y, Dai J, Liu C, et al. (2023): A higher dysregulation  
698 burden of brain DNA methylation in female patients implicated in the sex bias of  
699 Schizophrenia. *Mol Psychiatry*.
- 700 39. Klemmera P, Doubal S (2006): A new approach to the concept and computation of  
701 biological age. *Mech Ageing Dev*. 127:240-248.

- 702 40. Levine ME, Lu AT, Quach A, Chen BH, Assimes TL, Bandinelli S, et al. (2018): An  
703 epigenetic biomarker of aging for lifespan and healthspan. *Aging (Albany NY)*. 10:573-591.
- 704 41. Kwon D, Belsky DW (2021): A toolkit for quantification of biological age from blood  
705 chemistry and organ function test data: BioAge. *Geroscience*. 43:2795-2808.
- 706 42. Achenbach TM (2009): *The Achenbach system of empirically based assessment*  
707 *(ASEBA): Development, findings, theory, and applications*. Burlington: University of  
708 Vermont, Research Center for Children, Youth, and Families.
- 709 43. Marder SR, Davis JM, Chouinard G (1997): The effects of risperidone on the five  
710 dimensions of schizophrenia derived by factor analysis: combined results of the North  
711 American trials. *J Clin Psychiatry*. 58:538-546.
- 712 44. Kay SR, Fiszbein A, Opler LA (1987): The positive and negative syndrome scale  
713 (PANSS) for schizophrenia. *Schizophr Bull*. 13:261-276.
- 714 45. Montgomery SA, Asberg M (1979): A new depression scale designed to be sensitive  
715 to change. *Br J Psychiatry*. 134:382-389.
- 716 46. Young RC, Biggs JT, Ziegler VE, Meyer DA (1978): A rating scale for mania:  
717 reliability, validity and sensitivity. *Br J Psychiatry*. 133:429-435.
- 718 47. Hamilton M (1960): A rating scale for depression. *J Neurol Neurosurg Psychiatry*.  
719 23:56-62.
- 720 48. Griffanti L, Salimi-Khorshidi G, Beckmann CF, Auerbach EJ, Douaud G, Sexton CE,  
721 et al. (2014): ICA-based artefact removal and accelerated fMRI acquisition for improved  
722 resting state network imaging. *Neuroimage*. 95:232-247.
- 723 49. Robinson EC, Garcia K, Glasser MF, Chen Z, Coalson TS, Makropoulos A, et al.  
724 (2018): Multimodal surface matching with higher-order smoothness constraints. *Neuroimage*.  
725 167:453-465.

- 726 50. Braun U, Schafer A, Walter H, Erk S, Romanczuk-Seiferth N, Haddad L, et al.  
727 (2015): Dynamic reconfiguration of frontal brain networks during executive cognition in  
728 humans. *Proc Natl Acad Sci U S A*. 112:11678-11683.
- 729 51. Chen T, Cai W, Ryali S, Supekar K, Menon V (2016): Distinct Global Brain  
730 Dynamics and Spatiotemporal Organization of the Salience Network. *PLoS Biol*.  
731 14:e1002469.
- 732 52. Telesford QK, Lynall ME, Vettel J, Miller MB, Grafton ST, Bassett DS (2016):  
733 Detection of functional brain network reconfiguration during task-driven cognitive states.  
734 *Neuroimage*. 142:198-210.
- 735 53. Schaefer A, Kong R, Gordon EM, Laumann TO, Zuo XN, Holmes AJ, et al. (2018):  
736 Local-Global Parcellation of the Human Cerebral Cortex from Intrinsic Functional  
737 Connectivity MRI. *Cereb Cortex*. 28:3095-3114.
- 738 54. Petrican R, Fornito A (2023): Adolescent neurodevelopment and psychopathology:  
739 The interplay between adversity exposure and genetic risk for accelerated brain ageing. *Dev*  
740 *Cogn Neurosci*. 60:101229.
- 741 55. Petrican R, Fornito A, Boyland E (2023): Lifestyle Factors Counteract the  
742 Neurodevelopmental Impact of Genetic Risk for Accelerated Brain Aging in Adolescence.  
743 *Biol Psychiatry*.
- 744 56. Bazzi M, Porter MA, Williams S, McDonald M, Fenn DJ, Howison SD (2016):  
745 Community Detection in Temporal Multilayer Networks, with an Application to Correlation  
746 Networks. *Multiscale Modeling & Simulation*. 14:1-41.
- 747 57. Finc K, Bonna K, He X, Lydon-Staley DM, Kuhn S, Duch W, et al. (2020): Dynamic  
748 reconfiguration of functional brain networks during working memory training. *Nat Commun*.  
749 11:2435.

- 750 58. Gordon EM, Laumann TO, Adeyemo B, Huckins JF, Kelley WM, Petersen SE (2016):  
751 Generation and Evaluation of a Cortical Area Parcellation from Resting-State Correlations.  
752 *Cereb Cortex*. 26:288-303.
- 753 59. Bassett DS (2017): Network Community Toolbox.
- 754 60. Mucha PJ, Richardson T, Macon K, Porter MA, Onnela JP (2010): Community  
755 structure in time-dependent, multiscale, and multiplex networks. *Science*. 328:876-878.
- 756 61. Mattar MG, Cole MW, Thompson-Schill SL, Bassett DS (2015): A Functional  
757 Cartography of Cognitive Systems. *PLoS Comput Biol*. 11:e1004533.
- 758 62. Krishnan A, Williams LJ, McIntosh AR, Abdi H (2011): Partial Least Squares (PLS)  
759 methods for neuroimaging: a tutorial and review. *Neuroimage*. 56:455-475.
- 760 63. Escrichs A, Sanz Perl Y, Martinez-Molina N, Biarnes C, Garre-Olmo J, Fernandez-  
761 Real JM, et al. (2022): The effect of external stimulation on functional networks in the aging  
762 healthy human brain. *Cereb Cortex*. 33:235-245.
- 763 64. Mujica-Parodi LR, Amgalan A, Sultan SF, Antal B, Sun X, Skiena S, et al. (2020):  
764 Diet modulates brain network stability, a biomarker for brain aging, in young adults. *Proc*  
765 *Natl Acad Sci U S A*. 117:6170-6177.
- 766 65. Sastry NC, Roy D, Banerjee A (2023): Stability of sensorimotor network sculpts the  
767 dynamic repertoire of resting state over lifespan. *Cereb Cortex*. 33:1246-1262.
- 768 66. Stanford WC, Mucha PJ, Dayan E (2022): A robust core architecture of functional  
769 brain networks supports topological resilience and cognitive performance in middle- and old-  
770 aged adults. *Proc Natl Acad Sci U S A*. 119:e2203682119.
- 771 67. Hair JF, Black WC, Babin BJ, Anderson RE (2014): *Multivariate Data Analysis*. 7th  
772 Edition ed. Upper Saddle River: Pearson Education.
- 773 68. Sarkar A, Wrangham RW (2023): Evolutionary and neuroendocrine foundations of  
774 human aggression. *Trends Cogn Sci*. 27:468-493.

- 775 69. McTeague LM, Huemer J, Carreon DM, Jiang Y, Eickhoff SB, Etkin A (2017):  
776 Identification of Common Neural Circuit Disruptions in Cognitive Control Across Psychiatric  
777 Disorders. *Am J Psychiatry*. 174:676-685.
- 778 70. Dunlop BW, Cha J, Choi KS, Nemeroff CB, Craighead WE, Mayberg HS (2023):  
779 Functional connectivity of salience and affective networks among remitted depressed patients  
780 predicts episode recurrence. *Neuropsychopharmacology*. 48:1901-1909.
- 781 71. Javaheripour N, Li M, Chand T, Krug A, Kircher T, Dannlowski U, et al. (2021):  
782 Altered resting-state functional connectome in major depressive disorder: a mega-analysis  
783 from the PsyMRI consortium. *Transl Psychiatry*. 11:511.
- 784 72. Li J, Wang R, Mao N, Huang M, Qiu S, Wang J (2023): Multimodal and multiscale  
785 evidence for network-based cortical thinning in major depressive disorder. *Neuroimage*.  
786 277:120265.
- 787 73. Liu J, Fan Y, Ling-Li Z, Liu B, Ju Y, Wang M, et al. (2021): The neuroprogressive  
788 nature of major depressive disorder: evidence from an intrinsic connectome analysis. *Transl*  
789 *Psychiatry*. 11:102.
- 790 74. Sasabayashi D, Takahashi T, Takayanagi Y, Nemoto K, Ueno M, Furuichi A, et al.  
791 (2023): Resting state hyperconnectivity of the default mode network in schizophrenia and  
792 clinical high-risk state for psychosis. *Cereb Cortex*. 33:8456-8464.
- 793 75. Spronk M, Keane BP, Ito T, Kulkarni K, Ji JL, Anticevic A, et al. (2021): A Whole-  
794 Brain and Cross-Diagnostic Perspective on Functional Brain Network Dysfunction. *Cereb*  
795 *Cortex*. 31:547-561.
- 796 76. Wei W, Deng L, Qiao C, Yin Y, Zhang Y, Li X, et al. (2023): Neural variability in  
797 three major psychiatric disorders. *Mol Psychiatry*.
- 798 77. Yan W, Pearlson GD, Fu Z, Li X, Iraj A, Chen J, et al. (2024): A Brainwide Risk  
799 Score for Psychiatric Disorder Evaluated in a Large Adolescent Population Reveals Increased

- 800 Divergence Among Higher-Risk Groups Relative to Control Participants. *Biol Psychiatry*.  
801 95:699-708.
- 802 78. Beurel E, Toups M, Nemeroff CB (2020): The Bidirectional Relationship of  
803 Depression and Inflammation: Double Trouble. *Neuron*. 107:234-256.
- 804 79. Foley EM, Parkinson JT, Mitchell RE, Turner L, Khandaker GM (2023): Peripheral  
805 blood cellular immunophenotype in depression: a systematic review and meta-analysis. *Mol*  
806 *Psychiatry*. 28:1004-1019.
- 807 80. Sorensen NV, Orlovska-Waast S, Jeppesen R, Klein-Petersen AW, Christensen RHB,  
808 Benros ME (2022): Neuroinflammatory Biomarkers in Cerebrospinal Fluid From 106  
809 Patients With Recent-Onset Depression Compared With 106 Individually Matched Healthy  
810 Control Subjects. *Biol Psychiatry*. 92:563-572.
- 811 81. Zhang L, Zhao J, Zhou Q, Liu Z, Zhang Y, Cheng W, et al. (2021): Sensory,  
812 somatomotor and internal mentation networks emerge dynamically in the resting brain with  
813 internal mentation predominating in older age. *Neuroimage*. 237:118188.
- 814 82. Goodman ZT, Bainter SA, Kornfeld S, Chang C, Nomi JS, Uddin LQ (2021): Whole-  
815 Brain Functional Dynamics Track Depressive Symptom Severity. *Cereb Cortex*. 31:4867-  
816 4876.
- 817 83. Sun X, Sun J, Lu X, Dong Q, Zhang L, Wang W, et al. (2023): Mapping  
818 Neurophysiological Subtypes of Major Depressive Disorder Using Normative Models of the  
819 Functional Connectome. *Biological Psychiatry*. 94:936-947.
- 820 84. Baldassano C, Chen J, Zadbood A, Pillow JW, Hasson U, Norman KA (2017):  
821 Discovering Event Structure in Continuous Narrative Perception and Memory. *Neuron*.  
822 95:709-721 e705.

- 823 85. Chang CHC, Nastase SA, Hasson U (2022): Information flow across the cortical  
824 timescale hierarchy during narrative construction. *Proc Natl Acad Sci U S A*.  
825 119:e2209307119.
- 826 86. Petrican R, Soderlund H, Kumar N, Daskalakis ZJ, Flint A, Levine B (2019):  
827 Electroconvulsive therapy "corrects" the neural architecture of visuospatial memory:  
828 Implications for typical cognitive-affective functioning. *Neuroimage Clin*. 23:101816.
- 829 87. Baskin-Sommers A, Brazil IA (2022): The importance of an exaggerated attention  
830 bottleneck for understanding psychopathy. *Trends Cogn Sci*. 26:325-336.
- 831 88. Baskin-Sommers A, Ruiz S, Sarcos B, Simmons C (2022): Cognitive-affective  
832 factors underlying disinhibitory disorders and legal implications. *Nature Reviews Psychology*.  
833 1:145-160.
- 834 89. Viding E, McCrory E, Baskin-Sommers A, De Brito S, Frick P (2024): An 'embedded  
835 brain' approach to understanding antisocial behaviour. *Trends Cogn Sci*. 28:159-171.
- 836 90. Herniman SE, Wood SJ, Khandaker G, Dazzan P, Pariante CM, Barnes NM, et al.  
837 (2023): Network analysis of inflammation and symptoms in recent onset schizophrenia and  
838 the influence of minocycline during a clinical trial. *Transl Psychiatry*. 13:297.
- 839 91. Banaj N, Vecchio D, Piras F, De Rossi P, Bustillo J, Ciufolini S, et al. (2023): Cortical  
840 morphology in patients with the deficit and non-deficit syndrome of schizophrenia: a  
841 worldwide meta- and mega-analyses. *Mol Psychiatry*.
- 842 92. Lin X, Huo Y, Wang Q, Liu G, Shi J, Fan Y, et al. (2024): Using normative modeling  
843 to assess pharmacological treatment effect on brain state in patients with schizophrenia.  
844 *Cereb Cortex*. 34.
- 845 93. Zhou C, Tang X, Yu M, Zhang H, Zhang X, Gao J, et al. (2024): Convergent and  
846 divergent genes expression profiles associated with brain-wide functional connectome  
847 dysfunction in deficit and non-deficit schizophrenia. *Transl Psychiatry*. 14:124.

- 848 94. Segura AG, de la Serna E, Sugranyes G, Baeza I, Valli I, Diaz-Caneja C, et al. (2023):  
849 Epigenetic age deacceleration in youth at familial risk for schizophrenia and bipolar disorder.  
850 *Transl Psychiatry*. 13:155.
- 851 95. Hou C, Jiang S, Liu M, Li H, Zhang L, Duan M, et al. (2023): Spatiotemporal  
852 dynamics of functional connectivity and association with molecular architecture in  
853 schizophrenia. *Cereb Cortex*. 33:9095-9104.
- 854 96. Catalan A, McCutcheon RA, Aymerich C, Pedruzo B, Radua J, Rodriguez V, et al.  
855 (2024): The magnitude and variability of neurocognitive performance in first-episode  
856 psychosis: a systematic review and meta-analysis of longitudinal studies. *Transl Psychiatry*.  
857 14:15.
- 858 97. Holmes A, Levi PT, Chen YC, Chopra S, Aquino KM, Pang JC, et al. (2023):  
859 Disruptions of Hierarchical Cortical Organization in Early Psychosis and Schizophrenia. *Biol*  
860 *Psychiatry Cogn Neurosci Neuroimaging*. 8:1240-1250.
- 861 98. Rolls ET, Cheng W, Feng J (2021): Brain dynamics: the temporal variability of  
862 connectivity, and differences in schizophrenia and ADHD. *Transl Psychiatry*. 11:70.
- 863 99. Campbell IH, Campbell H (2024): The metabolic overdrive hypothesis:  
864 hyperglycolysis and glutaminolysis in bipolar mania. *Mol Psychiatry*. 29:1521-1527.
- 865 100. Solmi M, Soardo L, Kaur S, Azis M, Cabras A, Censori M, et al. (2023): Meta-  
866 analytic prevalence of comorbid mental disorders in individuals at clinical high risk of  
867 psychosis: the case for transdiagnostic assessment. *Mol Psychiatry*. 28:2291-2300.
- 868 101. de Lange SC, Scholtens LH, Alzheimer's Disease Neuroimaging I, van den Berg LH,  
869 Boks MP, Bozzali M, et al. (2019): Shared vulnerability for connectome alterations across  
870 psychiatric and neurological brain disorders. *Nat Hum Behav*. 3:988-998.
- 871 102. de Magalhaes JP (2024): Distinguishing between driver and passenger mechanisms of  
872 aging. *Nat Genet*. 56:204-211.



- 873 103. Cole JJ, McColl A, Shaw R, Lynall ME, Cowen PJ, de Boer P, et al. (2021): No  
874 evidence for differential gene expression in major depressive disorder PBMCs, but robust  
875 evidence of elevated biological ageing. *Transl Psychiatry*. 11:404.
- 876 104. Flynn LT, Gao WJ (2023): DNA methylation and the opposing NMDAR dysfunction  
877 in schizophrenia and major depression disorders: a converging model for the therapeutic  
878 effects of psychedelic compounds in the treatment of psychiatric illness. *Mol Psychiatry*.  
879 28:4553-4567.
- 880 105. Habets PC, Thomas RM, Milaneschi Y, Jansen R, Pool R, Peyrot WJ, et al. (2023):  
881 Multimodal Data Integration Advances Longitudinal Prediction of the Naturalistic Course of  
882 Depression and Reveals a Multimodal Signature of Remission During 2-Year Follow-up. *Biol*  
883 *Psychiatry*.
- 884 106. Lorenzo EC, Kuchel GA, Kuo CL, Moffitt TE, Diniz BS (2023): Major depression  
885 and the biological hallmarks of aging. *Ageing Res Rev*. 83:101805.
- 886 107. Ochi S, Roy B, Prall K, Shelton RC, Dwivedi Y (2023): Strong associations of  
887 telomere length and mitochondrial copy number with suicidality and abuse history in  
888 adolescent depressed individuals. *Mol Psychiatry*.
- 889 108. Protsenko E, Yang R, Nier B, Reus V, Hammamieh R, Rampersaud R, et al. (2021):  
890 "GrimAge," an epigenetic predictor of mortality, is accelerated in major depressive disorder.  
891 *Transl Psychiatry*. 11:193.
- 892 109. Akkouh IA, Ueland T, Szabo A, Hughes T, Smeland OB, Andreassen OA, et al.  
893 (2023): Longitudinal Transcriptomic Analysis of Human Cortical Spheroids Identifies Axonal  
894 Dysregulation in the Prenatal Brain as a Mediator of Genetic Risk for Schizophrenia. *Biol*  
895 *Psychiatry*.

- 896 110. Chen Y, Liu S, Zhang B, Zhao G, Zhang Z, Li S, et al. (2024): Baseline symptom-  
897 related white matter tracts predict individualized treatment response to 12-week antipsychotic  
898 monotherapies in first-episode schizophrenia. *Transl Psychiatry*. 14:23.
- 899 111. Kobayashi H, Sasabayashi D, Takahashi T, Furuichi A, Kido M, Takayanagi Y, et al.  
900 (2024): The relationship between gray/white matter contrast and cognitive performance in  
901 first-episode schizophrenia. *Cereb Cortex*. 34.
- 902 112. Lemke H, Klute H, Skupski J, Thiel K, Waltemate L, Winter A, et al. (2022): Brain  
903 structural correlates of recurrence following the first episode in patients with major  
904 depressive disorder. *Transl Psychiatry*. 12:349.
- 905 113. Zhu JD, Wu YF, Tsai SJ, Lin CP, Yang AC (2023): Investigating brain aging trajectory  
906 deviations in different brain regions of individuals with schizophrenia using multimodal  
907 magnetic resonance imaging and brain-age prediction: a multicenter study. *Transl Psychiatry*.  
908 13:82.
- 909 114. Anderson KM, Collins MA, Kong R, Fang K, Li J, He T, et al. (2020): Convergent  
910 molecular, cellular, and cortical neuroimaging signatures of major depressive disorder. *Proc*  
911 *Natl Acad Sci U S A*. 117:25138-25149.
- 912 115. Codeluppi SA, Xu M, Bansal Y, Lepack AE, Duric V, Chow M, et al. (2023):  
913 Prefrontal cortex astroglia modulate anhedonia-like behavior. *Mol Psychiatry*.
- 914 116. Cathomas F, Lin HY, Chan KL, Li L, Parise LF, Alvarez J, et al. (2024): Circulating  
915 myeloid-derived MMP8 in stress susceptibility and depression. *Nature*.
- 916 117. King S, Mothersill D, Holleran L, Patlola SR, Burke T, McManus R, et al. (2023):  
917 Early life stress, low-grade systemic inflammation and weaker suppression of the default  
918 mode network (DMN) during face processing in Schizophrenia. *Transl Psychiatry*. 13:213.

- 919 118. Rampersaud R, Protsenko E, Yang R, Reus V, Hammamieh R, Wu GWY, et al.  
920 (2022): Dimensions of childhood adversity differentially affect biological aging in major  
921 depression. *Transl Psychiatry*. 12:431.
- 922 119. Sumner JA, Colich NL, Uddin M, Armstrong D, McLaughlin KA (2019): Early  
923 Experiences of Threat, but Not Deprivation, Are Associated With Accelerated Biological  
924 Aging in Children and Adolescents. *Biol Psychiatry*. 85:268-278.
- 925 120. Sun Y, Fang J, Wan Y, Su P, Tao F (2020): Association of Early-Life Adversity With  
926 Measures of Accelerated Biological Aging Among Children in China. *JAMA Netw Open*.  
927 3:e2013588.
- 928 121. He Q, Wang W, Xu D, Xiong Y, Tao C, You C, et al. (2024): Potential causal  
929 association between gut microbiome and posttraumatic stress disorder. *Transl Psychiatry*.  
930 14:67.
- 931 122. Trujillo-Villarreal LA, Cruz-Carrillo G, Angeles-Valdez D, Garza-Villarreal EA,  
932 Camacho-Morales A (2024): Paternal Prenatal and Lactation Exposure to a High Caloric Diet  
933 Shapes Transgenerational Brain Macro and Microstructure Defects, Impacting Anxiety-like  
934 Behavior in Male Offspring Rats. *eNeuro*.
- 935 123. Jiang M, Tian S, Liu S, Wang Y, Guo X, Huang T, et al. (2024): Accelerated  
936 biological aging elevates the risk of cardiometabolic multimorbidity and mortality. *Nature*  
937 *Cardiovascular Research*. 3:332-342.
- 938 124. Graf GH, Crowe CL, Kothari M, Kwon D, Manly JJ, Turney IC, et al. (2022): Testing  
939 Black-White Disparities in Biological Aging Among Older Adults in the United States:  
940 Analysis of DNA-Methylation and Blood-Chemistry Methods. *Am J Epidemiol*. 191:613-  
941 625.
- 942 125. Walhovd KB, Lovden M, Fjell AM (2023): Timing of lifespan influences on brain and  
943 cognition. *Trends Cogn Sci*. 27:901-915.

- 944 126. Sanderson E, Glymour MM, Holmes MV, Kang H, Morrison J, Munafo MR, et al.  
945 (2022): Mendelian randomization. *Nat Rev Methods Primers*. 2.
- 946 127. Di Ianni T, Ewbank SN, Levinstein MR, Azadian MM, Budinich RC, Michaelides M,  
947 et al. (2024): Sex dependence of opioid-mediated responses to subanesthetic ketamine in rats.  
948 *Nat Commun*. 15:893.
- 949 128. Guo B, Zhang M, Hao W, Wang Y, Zhang T, Liu C (2023): Neuroinflammation  
950 mechanisms of neuromodulation therapies for anxiety and depression. *Transl Psychiatry*.  
951 13:5.
- 952 129. Jiang C, DiLeone RJ, Pittenger C, Duman RS (2024): The endogenous opioid system  
953 in the medial prefrontal cortex mediates ketamine's antidepressant-like actions. *Transl*  
954 *Psychiatry*. 14:90.
- 955 130. Johnston JN, Kadriu B, Kraus C, Henter ID, Zarate CA, Jr. (2024): Ketamine in  
956 neuropsychiatric disorders: an update. *Neuropsychopharmacology*. 49:23-40.
- 957 131. Kawatake-Kuno A, Li H, Inaba H, Hikosaka M, Ishimori E, Ueki T, et al. (2024):  
958 Sustained antidepressant effects of ketamine metabolite involve GABAergic inhibition-  
959 mediated molecular dynamics in aPVT glutamatergic neurons. *Neuron*.
- 960 132. Krystal JH, Kavalali ET, Monteggia LM (2024): Ketamine and rapid antidepressant  
961 action: new treatments and novel synaptic signaling mechanisms.  
962 *Neuropsychopharmacology*. 49:41-50.
- 963 133. Deng ZD, Robins PL, Regenold W, Rohde P, Dannhauer M, Lisanby SH (2024): How  
964 electroconvulsive therapy works in the treatment of depression: is it the seizure, the  
965 electricity, or both? *Neuropsychopharmacology*. 49:150-162.
- 966 134. Krystal JH, Kaye AP, Jefferson S, Girgenti MJ, Wilkinson ST, Sanacora G, et al.  
967 (2023): Ketamine and the neurobiology of depression: Toward next-generation rapid-acting  
968 antidepressant treatments. *Proc Natl Acad Sci U S A*. 120:e2305772120.

- 969 135. Mwilambwe-Tshilobo L, Setton R, Bzdok D, Turner GR, Spreng RN (2023): Age  
970 differences in functional brain networks associated with loneliness and empathy. *Netw*  
971 *Neurosci.* 7:496-521.
- 972 136. Wearn A, Tremblay SA, Tardif CL, Leppert IR, Gauthier CJ, Baracchini G, et al.  
973 (2024): Neuromodulatory subcortical nucleus integrity is associated with white matter  
974 microstructure, tauopathy and APOE status. *Nat Commun.* 15:4706.

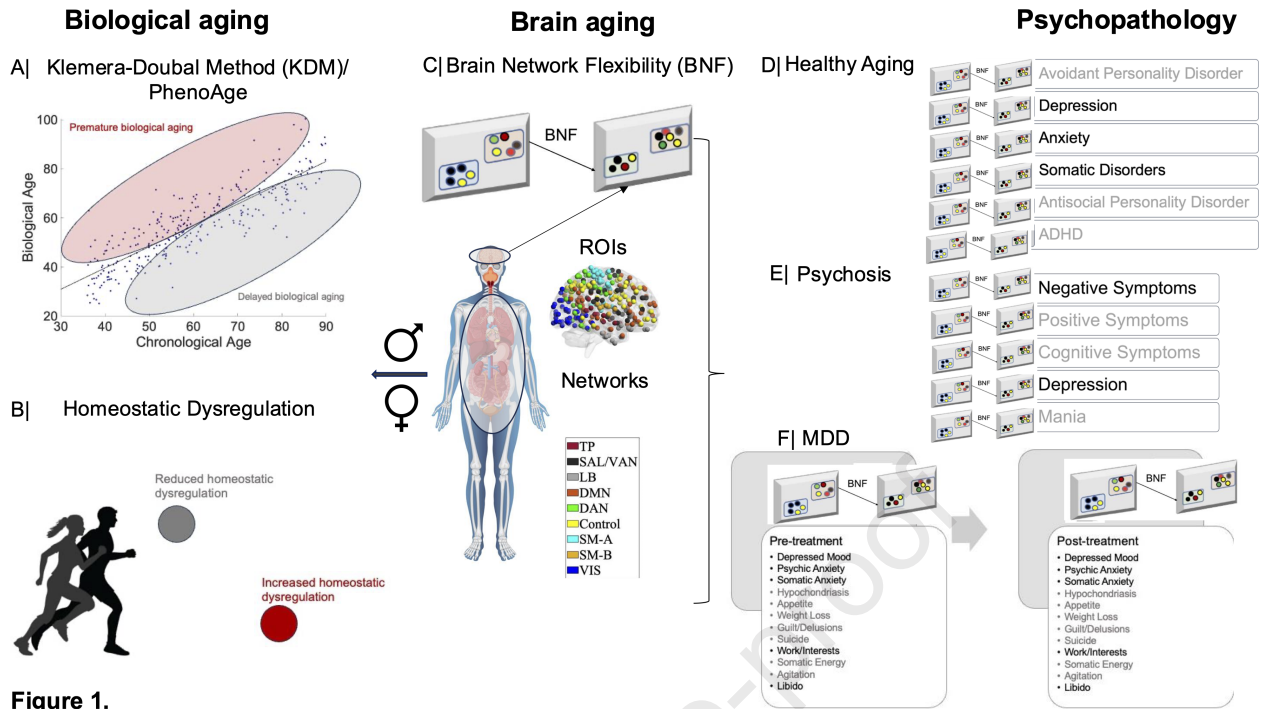


Figure 1.

## PLS 1: Intrinsic Brain Flexibility, Metabolic Aging and Sex

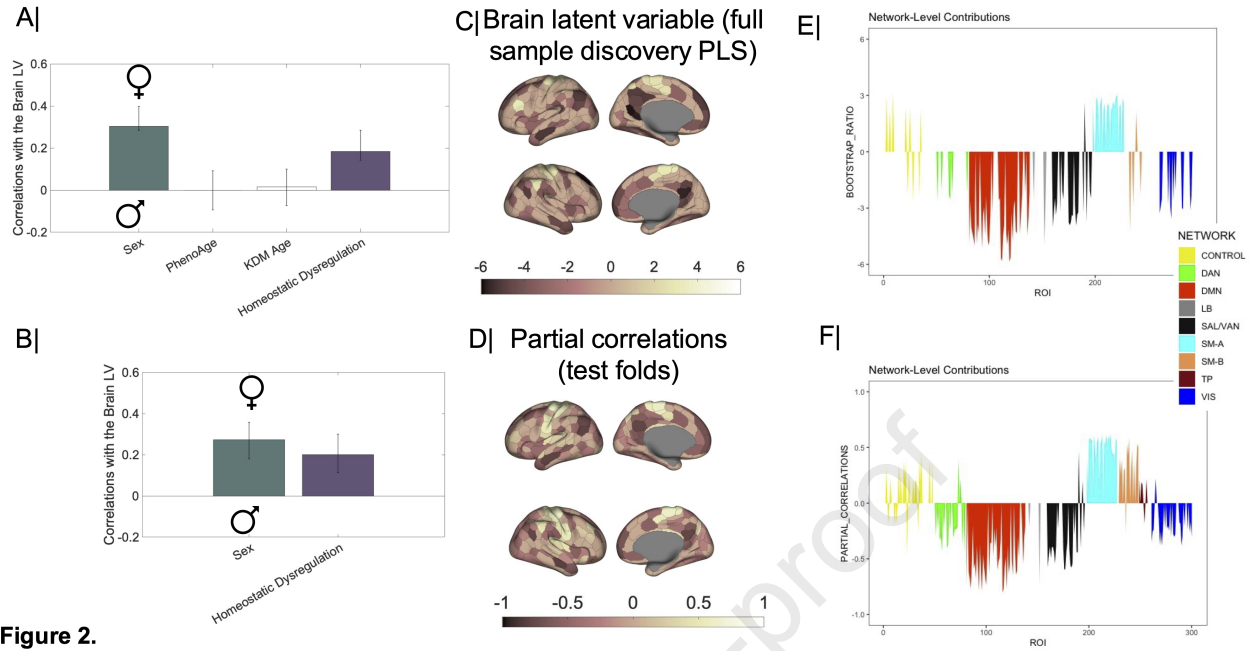
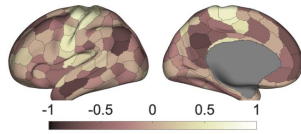


Figure 2.

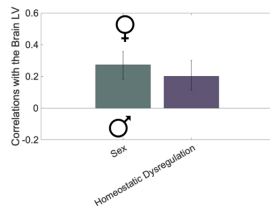
### CCA 1: Intrinsic Brain Network Flexibility Linked to Metabolic Aging and Psychiatric Disorder-Related Symptoms

#### A) Homeostatic Dysregulation-BNF Profile (HCP-A)



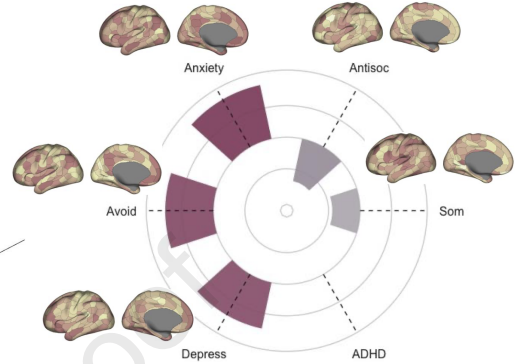
ROI BNF-Brain Latent Variable Correlations

$r = .72$ , permutation-based  $p = 10^{-6}$



#### B) Psychiatric Disorder-BNF Profile (HCP-A)

ROI BNF-Disorder Correlations



Loadings

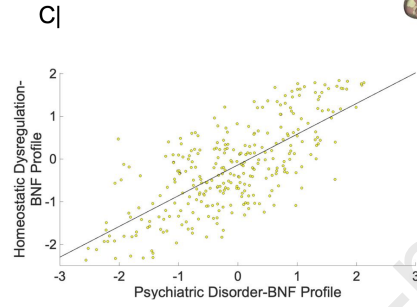
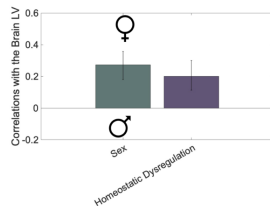
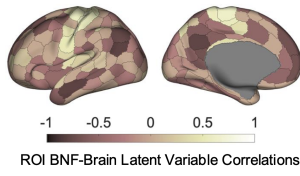


Figure 3.



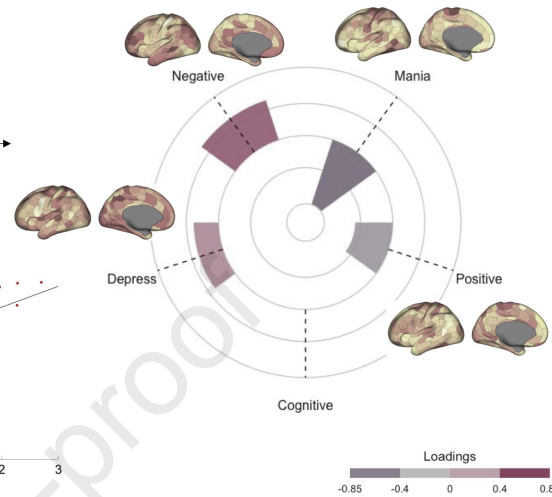
## CCA 2: Intrinsic Brain Network Flexibility Linked to Metabolic Aging and Psychotic Symptoms

## A| Homeostatic Dysregulation-BNF Profile (HCP-A)



## B| Psychotic Symptom-BNF Profile (HCP-EP)

ROI BNF-Symptom Correlations

 $r = .56$ , permutation-based  $p = 10^{-5}$ 

C|

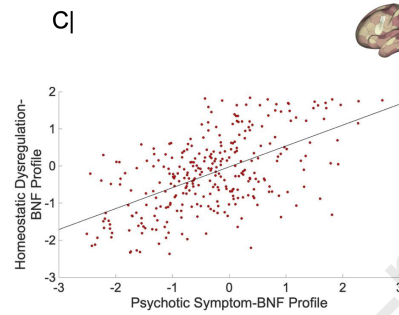
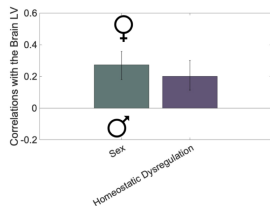
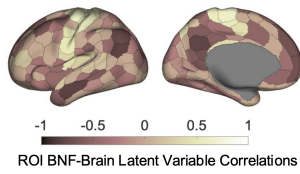


Figure 4.

### CCA 3: Intrinsic Brain Network Flexibility Linked to Metabolic Aging and Treatment-Related Resistance in MDD

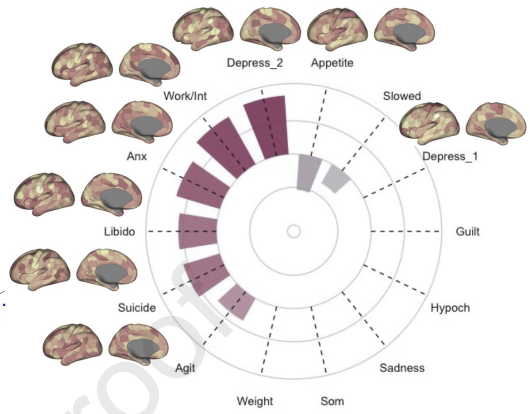
A) Homeostatic Dysregulation-BNF Profile (HCP-A)



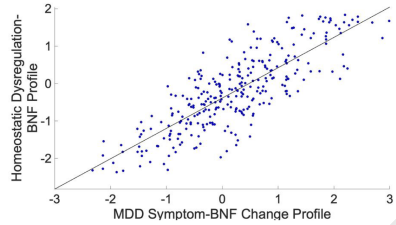
$r = .82$ , permutation-based  $p = 10^{-5}$

B) MDD Symptom-BNF Change Profile (PDC)

ROI BNF-Symptom (Change) Correlations



C)



Loadings

Figure 5.